Proceedings of the 2017 Winter Simulation Conference
W. K. V. Chan, A. D'Ambrogio, G. Zacharewicz, N. Mustafee, G. Wainer, and E. Page, eds.

HYBRID ADAPTIVE CONTROL FOR UAV DATA COLLECTION: A SIMULATION-BASED DESIGN TO TRADE-OFF RESOURCES BETWEEN STABILITY AND COMMUNICATION

Ezequiel Pecker Marcosig
Juan I. Giribet

Departamento de Ingeniería Electrónica
FI, UBA and CONICET
Av. Paseo Colón 850
C1063ACV, Buenos Aires, ARGENTINA

Rodrigo Castro

Departamento de Computación
FCEyN, UBA and ICC, CONICET
Ciudad Universitaria, Pabellón 1
C1428EGA, Buenos Aires, ARGENTINA

ABSTRACT

We present the design of a hybrid control system for an Unmanned Aerial Vehicle (UAV) used for data collection from wireless sensors. We postulate a restrictive scenario where a low-cost processor is in charge of both flying the UAV and resolving data communication. This raises the need for safe trade-off of computing resources between stability and throughput, adapting to unpredictable environment changes. We present a strategy where a supervisory controller implements an adaptive relaxation of the sampling period of the UAV regulation controller to favor communication tasks. To guarantee stability under period switching we update the discrete-time control law with suitable gains. The resulting system comprises continuous, discrete-time and discrete-event dynamics, including event-based adaptation of the discrete-time controller. We show how the DEVS modeling and simulation framework can support a full simulation-based design, verification and validation process, featuring a seamless composition of the underlying hybrid domains.

1 INTRODUCTION AND MOTIVATION

Hybrid feedback loops are pervasive in Cyber-Physical Systems (CPS) that integrate algorithmic and physical domains, as computational and physical processes influence each other. The uninterrupted operation of CPS under quality constraints is a key requirement for the discipline of hybrid control.

The overall quality of operation for a hybrid CPS must be guaranteed in the context of unpredictable dynamic environments including resource constraints. This can be achieved by orchestrating several self-adaptive capabilities of the CPS, under the responsibility of modularized cooperative controllers. Yet, the very notions of quality can differ drastically across domains. Core algorithmic concepts such as deadlocks or liveness are alien to the world of physics, while adherence to physical first principles such as the conservation of energy are seldom captured by computing abstractions. As a consequence, cooperative controllers are often organized in varied forms of hierarchical structures, which split responsibilities by distributing control tasks among well defined layers. This way, each type of controller can be designed by applying the best techniques available to that specific domain. Examples are model checking techniques for the verification of software implementing discrete-event controllers, and state space analysis of dynamic systems to design discrete-time controllers for continuous systems (Gokbayrak and Cassandras 2000).

Paradigmatic examples of interest in this work are data collection missions assigned to Unmanned Aerial Vehicles (UAV). In these scenarios a higher layer *supervisory control* deals with the reactive planning of convenient navigation paths and tasks, while a lower layer *regulation control* deals with driving the forces that maintain position, velocity and orientation of the vehicle (Karimoddini et al. 2014). Example applications are the monitoring of natural phenomena such as earthquakes or volcanic activity. In (Werner-Allen et al. 2005, Song et al. 2009) data collection and analysis aims to predict the occurrence of events and prevent human and material losses. Emergency scenarios such as firefighting (Ollero et al. 2007) require different data exchanges when the communication infrastructure is unavailable.

Inspired by these applications we consider a scenario where a number of wireless devices are randomly scattered on a field, and we need to collect data stored in them. Despite the success of previous approaches, new challenges arise when limited shared resources impose restrictions that compete with each other.

In order to reduce UAV costs, weight and size, a single on-board CPU can be shared to control a) the correct and stable flight of the UAV (subjected to perturbations, e.g. wind gusts) and b) the reliable collection of data from scattered devices (subjected to adverse conditions, e.g. fluctuating wireless channels). Depending on unpredictable environmental conditions a dynamic trade-off must be applied: maximize the effective throughput of data collection while minimizing the sacrificed stability.

When the UAV detects a patch with new sensors, it switches to a hovering state to allow for communication establishment and information retrieval. The UAV will hover until the transmission is completed. When more than one node is detected it is convenient that all available information is retrieved from all sensors within the range of coverage during the same hovering period. We shall consider that: a) the same on-board computer that executes the control algorithm which stabilizes the vehicle is also in charge of the communication and b) the computer has limited resources.

This creates a compromise between competing tasks: one needs resources to acquire information from nodes, while the other needs to execute the control algorithm often and fast enough to hold the vehicle in a desired position. Wind gusts produce transient responses in the UAV's angle. So a regulation control should counteract the effect of disturbances and keep the desired position of the UAV. We impose that the UAV should observe a certain degree of alignment with sensors on the land to establish an adequate communication, being the ideal condition when the UAV's is in hovering (hanging horizontal). Nevertheless, when it is sufficiently deviated from this ideal condition due to perturbations, the communication should be interrupted and restored after the transient response vanished.

The resulting competition for CPU resources between the supervisory control and the regulation control raises the need for a co-design of discrete-event, discrete-time and continuous controllers, i.e. a modular hybrid control design problem. The layered control approach calls for sound methodologies to assist the design process that allows for integrative testing of the controllers under a unified platform and in a safe way. In the particular case of UAVs, reducing testing risks and costs is mandatory.

Modeling and simulation-driven engineering has proven a successful strategy to support end-to-end designs of hybrid controllers (Castro et al. 2009). In order to achieve our goals, it is essential to count on an integrative framework that supports the interconnection of layered heterogeneous components in a seamless way. In this work we show how the DEVS (Discrete Event Systems Specification) framework (Zeigler et al. 2000) provides an efficient modeling paradigm and simulation mechanism to fulfill our requirements. We will present a case study for a simulation-assisted design, verification and partial validation of a hybrid control system for an UAV. The validation includes flying a real hexacopter subject to controlled maneuvers and a subsequent replication using trace-driven simulations.

The work is organized as follows. We first present our approach to tackle the stability vs. communication trade-off in Section 2. Section 3 presents key concepts on hybrid simulation and system stability. Section 4 describes the model for the UAV and the proposed adaptive control to stabilize the UAV under switching of the sampling period. The validity of the model implemented in PowerDEVS is partially evaluated in Section 5. Section 6 is devoted to the supervisory controller in charge of switching the sampling period for the UAV's attitude controller according to the number of sensors detected. The overall hybrid model is verified through simulation in Section 7. Finally, Section 8 presents conclusions and ideas for future work.

2 PROPOSED APPROACH: TRADE-OFF BETWEEN STABILITY AND COMMUNICATION

The approach we present here considers a supervisory controller which must be capable of: deciding how to reduce the sampling period of the attitude controller as a function of the number of detected sensors, guaranteeing the stability of the vehicle, to favor data acquisition and interrupting data collection while the UAV is being disturbed.

We subdivide the flight mission into stages according to the tasks (or modes) the UAV must perform. These are: *Take-off*, *Traveling*, *Hovering* and *Landing*. A mission starts with a *Take-off* phase. Then, during a *Traveling* phase the UAV scrutinizes the ground looking for sensors. While in *Hovering*, the UAV must retrieve data from the sensors detected in the previous step. We define that *Traveling* and *Hovering* phases are interleaved. Every mission ends with a *Landing* phase. The planning for an optimal coverage of the terrain during *Traveling* phases are out of the scope of this work.

Then, while in *Traveling* stage, we request a supervisory controller to select the *minimum achievable sampling period* (imposed by the electronics of the the UAV) for the regulation controller, which will be referred to as the *nominal period* h_0. Using this value the UAV exhibits the maximum control robustness to counteract wind disturbances, with controller using all CPU cycles to update the required forces. Yet, the UAV is only able to execute flight control tasks, and no data-retrieval can be performed.

When sensors are detected, the sampling period is relaxed ($h > h_0$) in order to assign some CPU resources to the communication task. The more relaxed (bigger) the period is, the more available CPU resources to upload data (which could translate into more sensors surveyed per mission given a fixed battery lifetime) at the expense of losing stability. Meanwhile, the sampling period is also upper-bounded with $h \leq h_{\max}$ by the UAV stability. In the case of a fixed bandwidth, $h_{\max}$ will determine the maximum number of sensors that can be simultaneously accessed.

Within the $h_0 < h < h_{\max}$ interval a suitable h must be selected in order to assign the optimal proportion of processor capacity according to the number of detected sensors. There exist guarantees that the vehicle can remain stable under sampling period switching, based on known results of control theory that provide us with explicit algebraic expressions to adapt the regulation controller.

During *Take-off* and *Landing* the regulation controller uses h_0 as no communication is required.

3 BACKGROUND

3.1 Hybrid Systems Modeling and Simulation with DEVS

Modeling and Simulation of hybrid systems is central to understand the behavior of discrete and continuous dynamics interacting with each other. This is because in most cases of practical interest hybrid systems don't accept analytical solutions.

DEVS is a formal model description framework equipped with an abstract simulation algorithm that is independent on the nature of the described system. It has been shown that DEVS can describe exactly any discrete system and approximate continuous systems with any degree of desired accuracy, therefore being capable to simulate all kinds of hybrid systems that undergo a finite amount of changes in finite intervals of time (Zeigler et al. 2000).

A system modeled with DEVS is described as a modular and hierarchical composite of submodels, each of them being behavioral (atomic) or structural (coupled). Submodels interact by means of events sent through input/output ports. A DEVS Atomic model is defined by the following tuple: $A = \{S, X, Y, \delta_{int}, \delta_{ext}, ta, \lambda\}$, where S is the set of internal states, X is the set of accepted external events, and Y is the set of available outputs. Four dynamic functions define behavior: $ta(s) : S \to \mathbb{R}_0^+$ is the lifetime of each state $s \in S$. After $ta(s)$ units of time an internal state transition $\delta_{int} : S \to S$ is triggered (assuming no external input events arrived). $\delta_{ext}(s, e, x) : S \times X \times \mathbb{R}_0^+ \to S$ is the external state transition function that is triggered when an input event arrives, with $0 \leq e < ta$ being the elapsed time in a given state. Every time a new state s' is selected with δ_{int} or δext, a new $ta(s')$ is calculated and the elapsed time e is reset. Finally, $\lambda(s) : S \to Y$ is the output function that can be invoked to send output events only when an internal transition is triggered.

An external transition is triggered every time an input in X is received. This change is performed instantaneously. On the other hand, the output function is executed when ta has elapsed since last event. Simultaneously, an internal transition is produced.

A DEVS Coupled model interconnects atomic and coupled components together through their input/output ports. It can be described by the following tuple: $C = \{X, Y, D, EIC, EOC, IC, Select\}$, where: X and Y are sets of input and output events respectively, D is the set of components names, IC is the set of internal couplings among members of D, EIC is the external inputs coupling relation (set of couplings between external input ports and internal components) and EOC is the external output coupling relation. *Select* is a tie-breaking function to assign execution priorities when several internal or external transition functions are scheduled for the same simulation time. The DEVS formalism is closed under coupling (i.e., any hierarchical coupling of DEVS atomic and coupled models defines an equivalent atomic DEVS model).

For practical modeling and simulation we adopted PowerDEVS (Bergero and Kofman 2010), an open-source simulation toolkit based on the DEVS formalism that is particularly oriented to hybrid systems. PowerDEVS is the flagship tool for the Quantized State System (QSS) family of numerical methods (Cellier and Kofman 2006) that solve differential equations efficiently in the context of a discrete-event simulation.

DEVS Graph provides a visual representation to describe the behavior of DEVS atomic models in a concise way. Each state $s \in S$ is indicated by a bubble with its name and lifetime, and arcs connecting bubbles denote state transitions. Dashed lines indicate internal transitions and solid lines indicate external transitions. The condition that must be satisfied by an input signal *In* to trigger an external transition when carrying a value *val* is indicated as: `In?val`. An output can only be produced after a state's lifetime has elapsed. An output of a *val* value on an *Out* port is indicated as: `Out!val`. We will use this notation to depict discrete-event behavior in Section 6.1 for supervisory controllers. The implementation of a DEVS model in PowerDEVS departing from a DEVS Graph diagram is straightforward.

3.2 Stability Analysis

Let $x(t) \in \mathbb{R}^n$ be a state vector whose evolution is described by a linear time-invariant system with input $u(t) \in \mathbb{R}^m$ as in (1), where $A \in \mathbb{R}^{n\times n}$ and $B \in \mathbb{R}^{n\times m}$ are the state and input matrices respectively. If we sample $x(t)$ by taking values at $t = kh$ for $k \in \mathbb{N}$ and sampling period $h > 0$, and assuming that $u(t)$ is constant between samples we obtain its discrete-time counterpart (2). There $x(k) = x(hk)$, $\Phi(h) = \exp(Ah) \in \mathbb{R}^{n\times n}$ and $\Gamma(h) = \int_0^h \exp(A\tau)\, d\tau B$, where $\exp : \mathbb{R}^{n\times n} \to \mathbb{R}^{n\times n}$ is the matrix exponential.

$$\dot{x}(t) = Ax(t) + Bu(t) \quad (1) \qquad x(k+1) = \Phi(h)x(k) + \Gamma(h)u(k) \quad (2) \qquad x(k+1) = \Phi^{CL}(h)x(k) \quad (3)$$

To control the system behavior we use state-feedback, that is $u(k) = K(h)x(k)$, where $K(h) \in \mathbb{R}^{m\times n}$ is the state-feedback gain which depends on the sampling period h. So closed loop equation is given by (3). The behavior of the state is determined by the closed-loop matrix $\Phi^{CL}(h) = \Phi(h) + \Gamma(h)K(h)$. Considering a finite set of admissible sampling periods $0 < h_0 < \cdots < h_N$, we have a family $\Sigma = \left\{\Phi_i^{CL}\right\}_{i=1,\ldots,N}$ of subsystems, where $\Phi_i^{CL} = \Phi^{CL}(h_i)$, $i = 0,...,N$. Thus, the evolution of $x(k)$ is a function of the active subsystem in Σ, which is time-dependent. Then, equation (3) can be seen as a linear autonomous Discrete-Time Switched System (DTSS):

$$x(k+1) = \Phi_{\sigma(k)}^{CL} x(k) \quad (4)$$

where $\sigma : \mathbb{N} \to \{0, \ldots, N\}$ is a piecewise constant function, which defines the switching sequence. In our case study the switching function σ is defined according to whether the UAV is retrieving data and the number of sensors which are being acquired. It is mandatory to guarantee the stability of the overall system for any possible switching sequence. In a switching system the stability of each individual subsystem is not a sufficient condition. As it was stated in (Narenda and Balakrishnan 1994) the commutativity between every pair of matrices in Σ ensures that a common quadratic Lyapunov function (CQLF) exists, and then the stability of the switching system is guaranteed. In (Felicioni and Junco 2008, Felicioni et al. 2010) the authors use this result to design adaptive control laws that guarantee stability for arbitrary switching sequences $\sigma(k)$. We shall rely on this result to adapt sampling periods dynamically with stability guarantees.

4 CONTINUOUS UAV MODEL AND DISCRETE REGULATION CONTROLLER

An UAV can be described as a rigid-body with six degrees of freedom ($6-DOF$). In particular for a multi-rotor vehicle, the position and its orientation are coupled. More specifically, to modify the lateral position of the vehicle it is necessary to modify its attitude. In fact, the attitude of the multi-rotor is the main variable to control, once the attitude is stabilized it is possible to control the vehicle position and eventually reject disturbances. The state vector $x(t) \in \mathbb{R}^6$ specifies the attitude of the vehicle: $x = \left[\phi, \dot{\phi}, \theta, \dot{\theta}, \psi, \dot{\psi}\right]^T$ as seen in Figure 1, where ϕ, θ and ψ are the pitch, roll and yaw angles, respectively. This rigid-body is subject to forces and moments: $u = \left[F_x, F_y, F_z, \tau_\phi, \tau_\theta, \tau_\psi\right]^T$. The dynamic equations which describe its movement are obtained by considering Euler-Newton equations (5)-(7) where $\mathbf{F}$ is the vector of forces (control input), $\mathbf{M}$ the moments vector (control input), $\mathbf{V}$ is the velocity of the vehicle, ω the angular velocity, m is the mass of the UAV and I is the inertia matrix. These quantities are expressed in the (non-inertial) vehicle frame. However, given the attitude of the vehicle (ϕ, θ, ψ) it is possible to refer the velocity of the UAV and its position in an inertial frame.

$$\begin{bmatrix} \dot{\phi} \\ \dot{\theta} \\ \dot{\psi} \end{bmatrix} = \begin{bmatrix} 1 & sin(\phi)tg(\theta) & cos(\phi)tg(\theta) \\ 0 & cos(\phi) & -sin(\phi) \\ 0 & \frac{sin(\phi)}{cos(\theta)} & \frac{cos(\phi)}{cos(\theta)} \end{bmatrix} \omega \tag{5}$$

$$m\dot{\mathbf{V}} = -\omega \times \mathbf{V} + \mathbf{F} \tag{6}$$

$$I\dot{\omega} = -\omega \times (I\omega) + \mathbf{M} \tag{7}$$

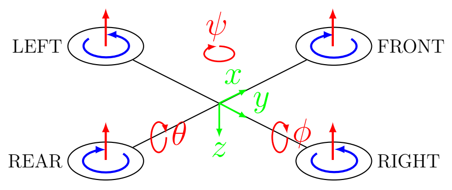

Figure 1: Schematic attitude angles.

This is a simplified model that does not take into account the behavior of actuators and sensors, but is good enough for the application studied in this work. For small angles near hovering, i.e. $\phi \simeq 0$, $\theta \simeq 0$, the non-linear model given in equations (5)-(7) can be linearized. This linearized model is commonly used to design the control algorithm for vehicles flying with standard maneuvers.

Moreover, the multi-rotor attitude model can be decomposed into three decoupled dynamical subsystems, one for each attitude angle, see Figure 1. For each of these angles we have a model like (8):

$$\dot{x}(t) = \begin{bmatrix} 0 & 1 \\ 0 & 0 \end{bmatrix} x(t) + \begin{bmatrix} 0 \\ b_0 \end{bmatrix} \tau(t) \tag{8}$$

$$x(k+1) = \left(\begin{bmatrix} 1 & h_i \\ 0 & 1 \end{bmatrix} + \begin{bmatrix} b_0 h_i^2/2 \\ b_0 h_i \end{bmatrix} K(h_i) \right) x(k) \tag{9}$$

where $b_0 = 1/I$ corresponds to the inverse of the inertia and $\tau(t) \in \mathbb{R}$ is the torque in the corresponding axis. State $x(t) \in \mathbb{R}^2$, represents the angle and angular velocity in the corresponding axis, for instance for pitch angle, $x = [\phi, \dot{\phi}]$. Following the ideas of Subsection 3.2, this model can be discretized. For each subsystem, a state-feedback controller is designed, such that: $\tau(k) = K(h_i)x(k)$, with $K(h_i) = \begin{bmatrix} K_1(h_i) & K_2(h_i) \end{bmatrix} \in \mathbb{R}^{1\times 2}$. Therefore, discrete-time closed-loop dynamics for each sampling period $h_i = 0, ..., N$ is given by (9) where the term in brackets is called Φ_i^{CL}.

Considering the different flight modes, the family of closed-loop matrices $\Sigma = \left\{\Phi_0^{CL}, \ldots, \Phi_N^{CL}\right\}$ should be stabilized for arbitrary switching. During a mission, a UAV acts as a data-mule and as it moves forward in its path it will be establishing communication with a different number of ground sensor nodes.

As it was mentioned in Section 3.2, ensuring stability for the system under arbitrary switching sequence is equivalent to asking for closed-loop matrices in Σ to be pairwise commutative. This approach can be easily applied by means of the algebraic equations:

$$K_1(h_i) = -4K_1(h_0)/\xi \quad , \quad K_2(h_i) = 2(h_0 K_1(h_0) - n h_0 K_1(h_0) - 2K_2(h_0))/\xi \tag{10}$$

with $n = h_i/h_0$ and $\xi = -4 + (n-1)b_0 h_0 (n h_0 K1(h_0) + 2K_2(h_0))$. Notice that, in order to calculate $K(h_i)$ for every $i = 1, ..., N$, we require to known $K(h_0)$. Of course, $K(h_0)$ should be such that $\Phi^{CL}(h_0)$ is stable.

For the sake of simplicity we will study only the case for the ϕ angle (pitch). As the dynamics of the angles can be decomposed and analyzed independently, our control strategy can be reused directly for the θ angle (roll). Dynamic associated with ψ angle (yaw) is slower than ϕ and θ so it is easier to deal with and thus we concentrate on pitch and roll.

In Figure 2 we can see how the adaptive discrete-time controller is connected to the UAV. Figure 3 shows our implementation of the system in PowerDEVS, using the adaptation law given in eq. (10).

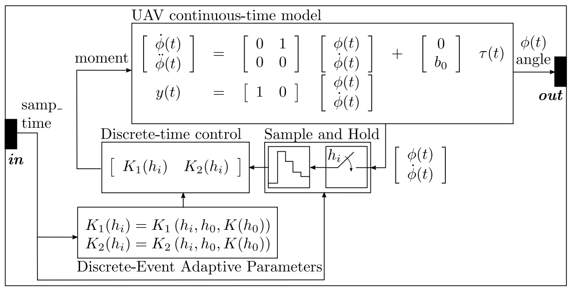
UAV continuous-time model
moment
$\begin{bmatrix}\dot\phi(t)\\ \ddot\phi(t)\end{bmatrix} = \begin{bmatrix}0&1\\0&0\end{bmatrix}\begin{bmatrix}\phi(t)\\ \dot\phi(t)\end{bmatrix} + \begin{bmatrix}0\\b_0\end{bmatrix}\tau(t)$
$y(t) = \begin{bmatrix}1&0\end{bmatrix}\begin{bmatrix}\phi(t)\\ \dot\phi(t)\end{bmatrix}$
$\phi(t)$ angle
out
samp_time
in
Discrete-time control
$\begin{bmatrix}K_1(h_i) & K_2(h_i)\end{bmatrix}$
Sample and Hold
h_i
$\begin{bmatrix}\phi(t)\\ \dot\phi(t)\end{bmatrix}$
$K_1(h_i) = K_1(h_i, h_0, K(h_0))$
$K_2(h_i) = K_2(h_i, h_0, K(h_0))$
Discrete-Event Adaptive Parameters

Figure 2: Continuous UAV system and its adaptive discrete-time/event controller (pitch angle)

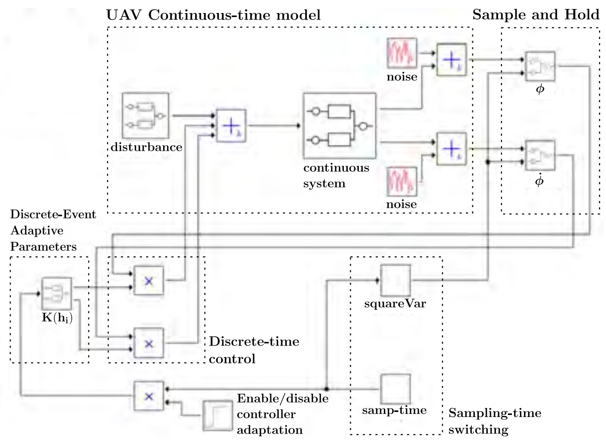

Figure 3: Hybrid system modeled in PowerDEVS. Dotted squares match blocks in Figure 2.

We will stress on the necessity of adapting the vehicle control law in a context of switching sampling period with the following simulated example. Let $h_0 = 5$ ms, $h_1 = 40$ ms, $h_2 = 290$ ms and the switching sequence σ followed by sampling period: h_0 over h_0, then h_1 for h_1 and finally h_2 during h_2. The sequence is repeated over time. If we do not conduct any adaptation, i.e. retain controller gains for h_0 called nominal gains hereafter, the result is an unbounded growth of the state values, i.e. an unstable system (see Figure 4). The matrix $\Phi^{CL}(h_0)\Phi^{CL}(h_1)\Phi^{CL}(h_2)$ has an unstable eigenvalue. Yet, each sampled subsystem is stable.

5 VALIDATION EXPERIMENTS

5.1 Experiments Performed with the UAV

In this section, we analyze a test carried out with an hexacopter emulating a flight mission. The vehicle and the autopilot (ChoriCopter) are developed in our labs (Pose et al. 2017). For this experiment we defined $h_0 = 5$ ms, $h_1 = 15$ ms and $h_2 = 25$ ms. In Figure 5 we can see the switching sequence followed by the sampling period driving the regulation controller. The UAV starts in *Take-off* mode and then switches to *Traveling* mode (both with h_0) following a predefined path to collect data. At 26 s the UAV detects a group of N_2 sensors. Thus, it evolves to *Hovering* mode and the supervisory controller assigns h_2 to the controller. Once data-retrieval is finished after about 15 s the UAV returns to *Traveling* and the supervisory controller switches the sampling period back to h_0. Around 58 s the vehicle detects a group of N_1 sensors and then jumps to *Hovering* again. In accordance with this value, the supervisory assigns h_1. The cycle of *Traveling* and *Hovering* modes with different sampling period is repeated. As it can be noticed from Figure 5, switching signal has some spurious glitches. This is due to some packets missed in the communication between the UAV and the computer used to monitor the experiment.

The measured *pitch angle* can be seen in Figure 6a. While in *Hovering* the angle reference is null whereas the current angle is not. This bias could be attributed to the lack of integral action in the regulation controller. The glitches around 22 s are related to the transition between *Take-off* and *Traveling* modes.

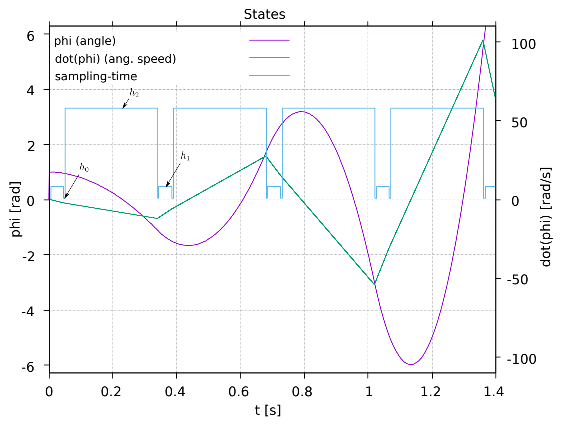

Figure 4: Continuous-state unstable behavior under sample-time switching.

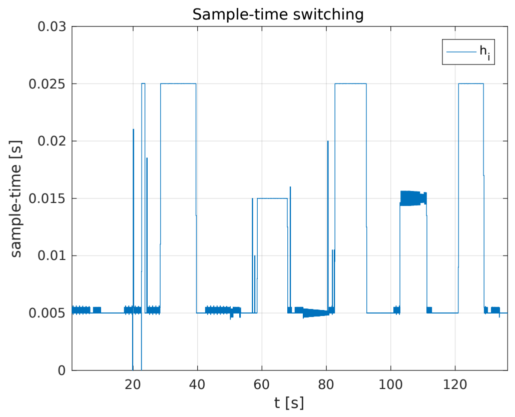

Figure 5: Manually-imposed sampling period.

5.2 Trace-Driven Simulation Validation

We used experimental data recorded during the tests in the previous section to validate our model implemented in PowerDEVS. We took the angle reference and sampling period signal traces to drive the simulation model. Figure 6b illustrates the resulting curves. Measured and simulated data are overlapped to check the degree of accuracy. The simulated angle follows the measured reference closely. However, measured and simulated pitch angles differ in an offset. Even without capturing this effect in our model, we conclude that the approximation is quite acceptable for our purposes. Having verified the validity of the hybrid model in Figure 3 for the lower layer, we are ready to further develop the supervisory controller on the higher layer.

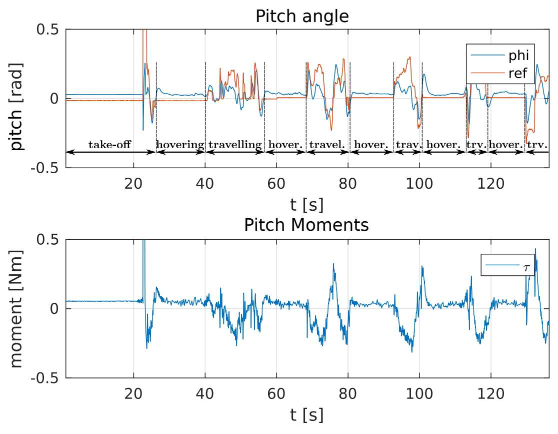

(a) Measured pitch angle and moment.

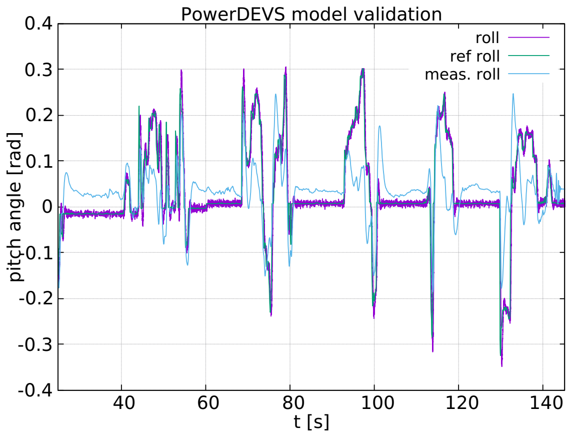

(b) Pitch angle comparison between 25 s and 145.2 s.

Figure 6: Evolution of measured and simulated $\phi(t)$ during an experiment.

6 SUPERVISORY CONTROL DESIGN: DISTURBANCE REJECTION VS. COMMUNICATION EFFICIENCY

The strategy followed here to implement the trade-off mentioned in Section 2 is to increase the sampling period of the vehicle controller, when needed, so as to have more time to acquire information. The amount of time necessary to execute the control task T_{ctrl} is determined by the CPU and is a fixed value. The sampling period used during the *Traveling* stage, when no data is being collected, equals this value. The time elapsed between two consecutive executions of the control task is the sampling-period. It can be subdivided into one part when the CPU is devoted to execute control task and the remainder where it is used to collect data. If we limit the time while the UAV is collecting data not to waste energy, we will need to enlarge the sampling period so as to collect a bigger amount of data. The previous trade-off is then expressed as the relation between the sampling period and its part devoted to data acquisition.

We discussed already that we can't use always the minimum value for sampling period T_{ctrl} because with this value no data can be collected. But, why don't we always use the maximum value, $h_{\max}$? The reason is that disturbance rejection in this case is the worst that can be achieved.

The UAV is required to remain hovering collecting data for a time $\bar{T}$, no matter how many sensors the UAV has to communicate to. This time limit is set in order to rationalize energy consumption, and is valid only in the absence of disturbances. Otherwise it will take longer than $\bar{T}$ to collect a same amount of data.

Once a communication protocol between the UAV and the sensors is defined, the bandwidth BW gets fixed. Thus, the time needed to collect all data by a group of N sensors is given by (11), where L_{msg} is the message length and $T_{tx} < \bar{T}$. During this time the CPU is exclusively devoted to data acquisition, and the remainder $\bar{T} - T_{tx}$ is used for the vehicle controller execution. The number of sampling periods that fit within $\bar{T}$ is $n_{msg} \in \mathbb{N}_0$, and it is calculated as in (12). This is the number of executions of the vehicle controller conducted while performing the overall data transmission.

$$T_{tx} = \frac{NL_{msg}}{BW} \qquad (11) \qquad\qquad n_{msg} = \frac{\bar{T} - T_{tx}}{T_{ctrl}} \qquad (12) \qquad\qquad h_i = T_{ctrl} + \frac{T_{tx}}{n_{msg}} \qquad (13)$$

The sampling period for the regulation controller is obtained from the expression in (13). This value represents the minimum sampling period needed to collect all data in time $\bar{T}$. If the sampling period were longer than this all data could be gathered in a shorter time but at the expense of being less robust to disturbances. Finally, the portion of a single h_i devoted to data acquisition is given by $T_{meas} = h_i - T_{ctrl}$.

The data communication efficiency η_{data} is the ratio between the fraction of the sampling period used for data collection and the sampling period itself. But on the other hand, it is also the quotient between the time during which the UAV is required to be in hovering and T_{tx}: $\eta_{data} = T_{meas}/h_i = T_{tx}/\bar{T}$. Its value is bounded by $0 \leq \eta_{data} \leq \bar{\eta}_{data} < 1$, since the sampling period is limited by $T_{ctrl} \leq h_i \leq h_{\max}$. Finally, the expression in (14) relates sampling period with the number of sensors N. Since h_i is upper bounded by $h_{\max}$, then this value determines $N_{\max}$. Let $\xi = \bar{T}BW/L_{msg}$, then

$$h_i = \begin{cases} T_{ctrl}\xi/(\xi - N) & \text{if } 0 \leq N \leq N_{\max} \\ T_{ctrl}\xi/(\xi - N_{\max}) & \text{otherwise} \end{cases} \qquad (14)$$

6.1 DEVS Model Specification

The DEVS Graph corresponding to the Transient Detector is shown in Figure 7a. This block acts as an interface between continuous and discrete states. The input of this detector is the UAV angle, whereas its output is a binary signal indicating whether the UAV is undergoing a transient response. This output feeds the Supervisory Controller. The Transient Detector starts in the **out** state, indicating that deviation from hovering is outside preestablished bounds set by L_limit and U_limit parameters, respectively. The state remains in **out** until a new angle information lies within bounds. In that case, an external transition is triggered and the state jumps to **wait**. There, it waits for a predefined stabilization time δ after which an internal transition is triggered, changing its state to **in** and outputting an IN_TRAN signal. If while in the **wait** state the angle input falls outside bounds, an external transition would jump back to **out** state but producing an OUT_TRAN output. Once in the **in** state, it remains there while the angle is inbound. Otherwise, an internal transition would switch state to **out** and produce an OUT_TRAN output.

This controller was implemented as a DEVS coupled model. It consists of an in/out band detector, made of two comparators, and the Transient Detector itself which is a DEVS atomic model.

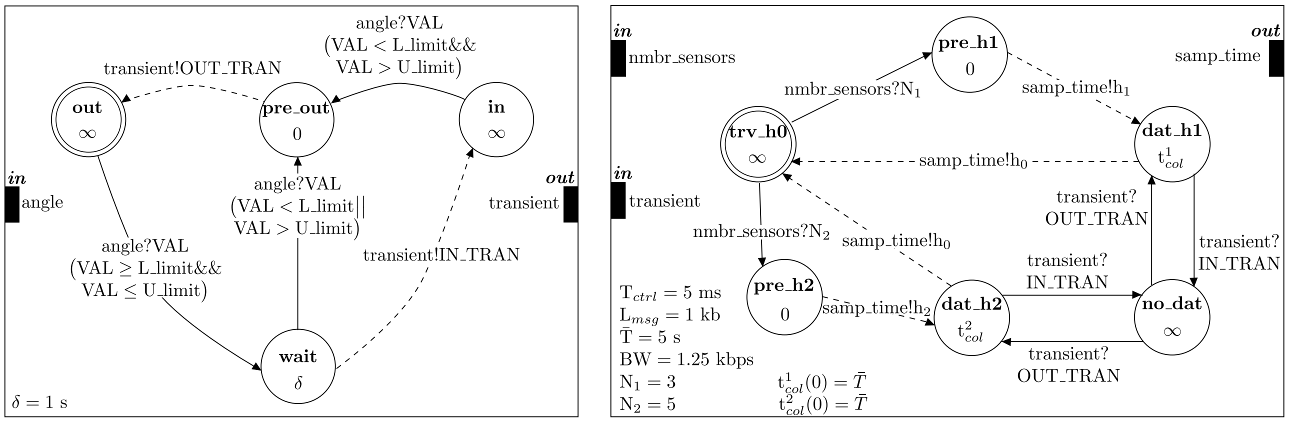

(a) Transient response detector

(b) Supervisory controller

Figure 7: Communication and processing resources allocator unit.

Figure 7b exhibits a DEVS Graph representation of the Supervisory Controller, defined by a DEVS atomic model with two inputs and one output. The first input receives a signal provided by the Transient Detector to decide weather angle conditions are met to collect data. The second input receives the number of detected sensors. For the present case, this can take values: 0, N_1 or N_2. Every time a group of sensors is detected, an input to this atomic model is produced. The supervisory controller then decides which sampling period should be used: h_0, h_1 or h_2 and outputs this value through its corresponding output port.

```
S :  {trv_h0, pre_h1, pre_h2, dat_h1, dat_h2, no_dat, sigma}
X :  {(nmbr_sensors, {N1, N2});
         (transient, {IN_TRAN, OUT_TRAN})}
Y :  {(samp_time, {h0, h1, h2})}
δint(s) :  if (s == pre_h1){ // Internal Transition
               s = dat_h1;
               h = h1;
               sigma = Tbar;}
           else if (s == pre_h2){
               s = dat_h2;
               h = h2;
               sigma = Tbar;}
           else if (s == dat_h1) {
               s = trv_h0;
               h = h0;
               sigma = INF;}
           else if (s == dat_h2) {
               s = trv_h0;
               h = h0;
               sigma = INF;}
δext(s,e,x)  :  if (x.port == 0){ // External Transition
               if ((s == trv_h0)&&(*xv == N1)){
                   s = pre_h1;
                   sigma = 0;}
               if ((s == trv_h0)&&(*xv == N2)){
                   s = pre_h2;
                   sigma = 0;}}
           if (x.port == 1){
               if ((s == dat_h1)&&(*xv == 0)){
                   elapsed_h = e;
                   s = no_dat;
                   sigma = INF;}
               if ((s == dat_h2)&&(*xv == 0)){
                   elapsed_h = e;
                   s = no_dat;
                   sigma = INF;}
               if ((s == no_dat)&&(*xv == 1)){
                   if (h == h1) {
                       s = dat_h1;
                       sigma = Tbar - elapsed_h;}
                   if (h == h2){
                       s = dat_h2;
                       sigma = Tbar - elapsed_h;}}}
λ(s) :     if (s == pre_h1){ // Output
               y[0] = h1;}
           else if (s == pre_h2){
               y[0] = h2;}
           else if ((s == dat_h1) || (s == dat_h2)){
               y[0] = h0;}
           else if (s == trv_h0){
               y[0] = h0;
               sigma = INF;}
           return Event(&y,0)
ta(s) :    return sigma // Time advance
```

Figure 8: Pseudocode for the *Superv_Ctrl* DEVS Atomic Model.

The Supervisory Controller starts in **trv_h0** state (*Traveling* phase defined in Section 2). Depending on the number of sensors detected, N_1 or N_2, the state jumps to **dat_h1** or **dat_h2** respectively. Before reaching these states, the corresponding sampling period computed with (14) is outputted. The Supervisory Controller will remain in either **dat_h1** or **dat_h2** while the UAV is collecting data, for t_{col}^1 or t_{col}^2 units of time. In absence of disturbances, these variables equal $\bar{T}$. Otherwise, if a disturbance is experienced strong enough to take the angle out of bounds, an external transition to **no_dat** state is produced. When the

Transient Detector indicates that deviation from hovering is considerable then data acquisition is stopped. After resuming from **no_dat**, the acquisition in either **dat_h1** or **dat_h2** continues for the difference between $\bar{T}$ and the elapsed time before the transient took place. In this case, the time needed to collect all stored data gets longer. Once all the information is acquired, an internal transition is produced and the supervisory state jumps back to **trv_h0**, with sampling period h_0. The controller in Figure 7b is formally defined as a DEVS atomic model $Superv\_Ctrl = \{S, X, Y, \delta_{int}, \delta_{ext}, t_a, \lambda\}$ whose pseudocode can be seen in Figure 8.

Figure 9 illustrates the resulting overall hybrid DEVS model structure. The **Supervisory Controller Unit for Resources Allocation** at the top has an input to receive the number of detected sensors. The output port of this block is connected to the **Continuous Dynamic** block at the bottom. Through this connection the current sampling period is sent to the adaptive discrete-time regulation controller. This is also an event-based signal. The output from the Regulation Controller is the continuous moment applied to the UAV by the actuators. The tilt angle, which is also a continuous signal, is connected to the Transient Detector. Finally, the transient detector output is also an event-based signal.

7 SIMULATION RESULTS

We performed tests on the model of Figure 9 considering the values shown in Table 1. The data collection efficiency is bounded by $0 \leq \eta_{data} \leq 0.8$. Figure 10 illustrates the sampling period in (14) for $N \in [0, 10]$. With these parameters, groups of sensors larger than 5 saturate the sampling period.

Verification in absence of disturbances. Figure 11a illustrates the results of this simulation. The UAV starts *Traveling*. At $t = 10$ s it detects a group of N_2 sensors. It takes $\bar{T}$ to collect all data from them in *Hovering* stage. After finishing, the UAV switches to *Traveling* again. At $t = 25$ s, the vehicle detects N_1 sensors. It switches to *Hovering* and takes $\bar{T}$ again to collect all data. After that, it travels between 32.5 s and 60 s. At $t = 60$ s and 85 s, N_2 and N_1 are detected respectively. Each sample period switch is followed by an execution of the adaptation algorithm (Eq.10).

Verification considering disturbances. Figure 11b shows the same experiment but now carried out in the presence of disturbances. These are represented by momentum pulses which emulate a sudden wind gust. We simulate the influence of three different disturbance durantions and amplitudes.

Disturbances d appear at 5 s, 63 s and 87 s (and last until 7 s, 66 s and 92 s) while the vehicle regulation controller is using h_0, h_2 and h_1 respectively. That means that the first and second data acquisition (*Hovering*) phases (between 10 s and 15 s and between 25 s and 30 s) are performed without being altered by wind. Disturbances cause a transient response in the angle of the UAV. Depending on the intensity of the gusts, the angle response can escape from the stability band limited by U_limit and L_limit, making the supervisory controller to stop data acquisition. These limits are shown in Figure 11b (bottom pane) with dashed lines. When the angle returns within the band for a time longer than δ the supervisor resumes data acquisition.

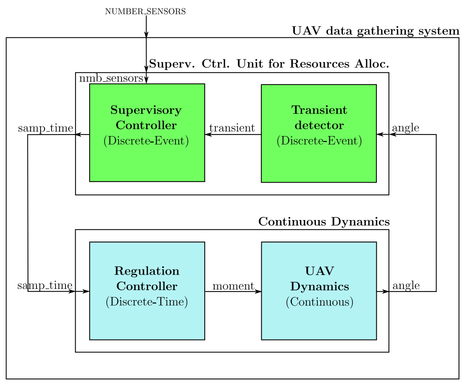
NUMBER_SENSORS
UAV data gathering system
Superv. Ctrl. Unit for Resources Alloc.
nmb_sensors
Supervisory Controller (Discrete-Event)
transient
Transient detector (Discrete-Event)
samp_time
angle
Continuous Dynamics
Regulation Controller (Discrete-Time)
moment
UAV Dynamics (Continuous)
samp_time
angle

Figure 9: Hybrid system for CPU allocation under stability constraints.

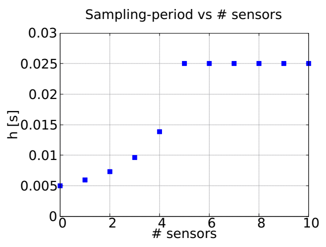

Figure 10: Sampling period vs. number of sensors.

Parameter	Value
BW	1.25 kbps
L_{msg}	$1kb$
$\bar{T}$	5 s
T_{ctrl}	5 ms
$h_{\max}$	25 ms
N_1	3
N_2	5
U_limit	0.2 rad
L_limit	-0.2 rad
δ	1 s

Table 1: Parameter values used for testing.

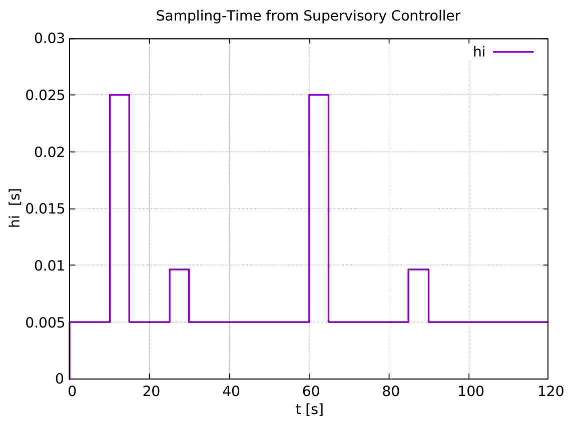

(a) Without disturbances

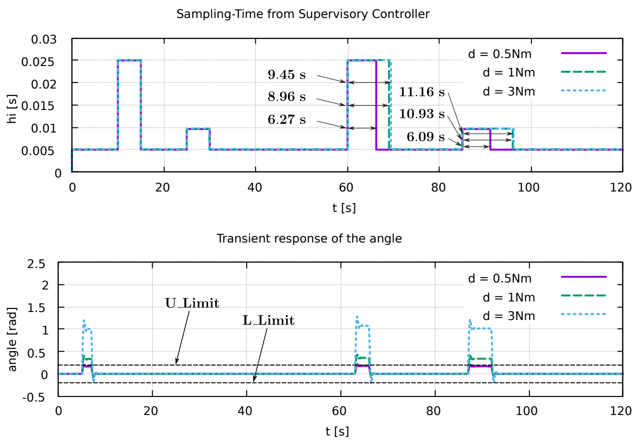

(b) Considering disturbances

Figure 11: Sampling period during acquisition.

The effects of disturbances in the third and fourth acquisitions are clearly seen in Figure 11b (upper pane) where the width of the hovering periods vary according to the strength and length of each disturbance.

It can be concluded that the stronger and longer the disturbance the longer the time used to collect all data. Also, the higher the sampling period, the less robust the system becomes to a same disturbance, which implies bigger transient response amplitudes and longer settling times. This highlights the necessity to relax the controller sampling period only when necessary and no more than strictly required.

8 CONCLUSIONS AND FUTURE WORK

We presented a modeling and simulation-assisted design of a hybrid supervisory controller for an unmanned aerial vehicle (UAV) collecting data from scattered wireless sensors. The UAV requires to allocate scarce CPU capacity under competing cyber-physical constraints: stability vs. data communication. A supervisory control layer resorts to sampling period relaxation of the regulation control layer. To guarantee stability we consider an adaptation of the control law that allows to update safe control gains. The continuous dynamics of the UAV physics are modelled with differential equations. A discrete-time PI controller is implemented to fly and stabilize the UAV in the presence of disturbances. Two kinds of discrete events are considered, driven by unpredictable dynamics: the detection of new sensors and the intervention of wind.

We proposed a control mechanism to trade-off processor resources between stability and communication constraints, setting bounds for the UAV angles within which communication quality is acceptable. The combined dynamics yield unpredictable sequences of discrete events. The strategy based on sample period adaptation for the regulation controller demanded extra guarantees of stability. Thus, depending on discrete-event dynamics, we adapt the discrete-time dynamics that affect the stability of the continuous part. We successfully followed a modeling and simulation-driven engineering approach relying on the DEVS framework to compose hybrid domains in a seamless way. We achieved model continuity and iterative system design. We smoothly used the same DEVS models and simulator to a) verify the hypothesis of destabilization of the continuous system under certain sampling period switchings, b) validate the continuous model under switching conditions by flying a real hexacopter, driving simulations with real recorded traces, c) design an event-based control to adapt the discrete-time controller with stability guarantees, and d) verify scenarios where a varying number of sensors and wind conditions create competition for CPU.

Our design leaves room for several improvements. One option is to add a time-limit for the **no_dat** state of the supervisory level so that the controller can choose a lower sampling period to reduce the number of sensors accessed simultaneously. This can improve the rejection of disturbances, but can also increase the time to collect all data (the supervisory controller should select a smaller group of sensors). The new aim would be not to waste time trying to collect all possible data since sensors might exhibit spatial correlation. We will also explore supervisory controller synthesis to guarantee deadlock-free operation.

REFERENCES

Bergero, F., and E. Kofman. 2010. "PowerDEVS: A Tool for Hybrid System Modeling and Real-Time Simulation". *SIMULATION* 87 (1-2): 113–132.

Castro, R., E. Kofman, and G. Wainer. 2009. "A DEVS–based End-to-end Methodology for Hybrid Control of Embedded Networking Systems". *IFAC Proceedings Volumes* 42 (17): 74–79.

Cellier, F. E., and E. Kofman. 2006. *Continuous System Simulation*. Springer Science. & Business Media.

Felicioni, F., C. Berbra, S. Gentil, and S. Lesecq. 2010. "On-line Adaptive Control of a Quadrotor under (m,k)-Firm Constraint". In *XXII Congreso Argentino de Control Automático AADECA 2010, Buenos Aires, Argentina*. AADECA.

Felicioni, F. E., and S. J. Junco. 2008. "A Lie Algebraic Approach to Design of Stable Feedback Control Systems with Varying Sampling Rate". *IFAC Proceedings Volumes* 41 (2): 4881–4886.

Gokbayrak, K., and C. G. Cassandras. 2000. "Hybrid Controllers for Hierarchically Decomposed Systems". In *Hybrid Systems: Computation and Control*, 117–129. Springer Berlin Heidelberg.

Karimoddini, A., H. Lin, B. M. Chen, and T. H. Lee. 2014. "Hierarchical Hybrid Modelling and Control of an Unmanned Helicopter". *International Journal of Control* 87 (9): 1779–1793.

Narenda, K. S., and J. Balakrishnan. 1994. "A Common Lyapunov Function for Stable LTI Systems with Commuting A-Matrices". *IEEE Transactions on Automatic Control* 39 (12): 2469–2471.

Ollero, A., P. J. Marron, M. Bernard, J. Lepley, M. la Civita, E. de Andres, and L. van Hoesel. 2007. "AWARE: Platform for Autonomous Self-Deploying and Operation of Wireless Sensor-Actuator Networks Cooperating with Unmanned Aerial Vehicles". In *Safety, Security and Rescue Robotics, 2007. SSRR 2007. IEEE International Workshop on*, 1–6. IEEE.

Pose, C., J. Giribet, and A. Ghersin. 2017. "Hexacopter Fault Tolerant Actuator Allocation Analysis for Optimal Thrust". In *2017 International Conf. on Unmanned Aircraft Systems (ICUAS)*, 663–671: IEEE.

Song, W.-Z., R. Huang, M. Xu, A. Ma, B. Shirazi, and R. LaHusen. 2009. "Air-Dropped Sensor Network for Real-Time High-Fidelity Volcano Monitoring". In *Proceedings of the 7th International Conf. on Mobile Systems, Applications, and Services*, 305–318. ACM.

Werner-Allen, G., J. Johnson, M. Ruiz, J. Lees, and M. Welsh. 2005. "Monitoring Volcanic Eruptions with a Wireless Sensor Network". In *Proceeedings of the Second European Workshop on Wireless Sensor Networks, 2005.*, 108–120. IEEE.

Zeigler, B. P., H. Praehofer, and T. G. Kim. 2000. *Theory of Modeling and Simulation: Integrating Discrete Event and Continuous Complex Dynamic Systems*. 2 ed. Academic press.

AUTHOR BIOGRAPHIES

EZEQUIEL PECKER MARCOSIG is an Electronics Engineer and a PhD student in the Facultad de Ingeniería, Universidad de Buenos Aires. His research interests include automatic control, discrete-event simulation, wireless networked control systems and hybrid systems. His e-mail address is epecker@fi.uba.ar.

JUAN I. GIRIBET is a Professor at the Universidad of Buenos Aires, and director of the Master degree in Mathematical Engineering. He is also a researcher at CONICET. His research interests are operator theory and its applications to control theory and signal processing. His e-mail address is jgiribet@fi.uba.ar.

RODRIGO CASTRO is a Professor in the Departamento de Computación, Facultad de Ciencias Exactas y Naturales, Universidad de Buenos Aires, head of the Simulation Lab, and a researcher at CONICET. His research interests include simulation and control of hybrid systems. His email address is rcastro@dc.uba.ar.